6, 714 (1986); A. Cacéres, G. A. Banker, O. Steward, L. I. Binder, M. Payne, *Dev. Brain Res.* **13**, 314 (1984); P. De Camilli, P. E. Miller, F. Navone, W. E. Theurkauf, R. B. Vallee, *Neuroscience* **11**, 819 (1984); C. G. Dotti, G. A. Banker, L. I. Binder, *ibid.* **23**, 121 (1987).
22. Hippocampal neurons were labeled with 20 n*M* TmRhd–ω-CgTx in medium A (*20*). After 45 min at 21°C the cells were washed with medium A. Sequential phase and fluorescence images of the same field were obtained on-line with a Hamamatsu Photonics VIM camera mounted onto a Zeiss Photomicroscope III and through a ×63 water-immersion objective with a numerical aperture of 1.2. The 514-nm line of an attenuated and dispersed argon laser beam served as the illumination source for fluorescence images. Because of the low emission from fluorescence images, the intensifier of the camera was operated in the photon counting mode. Image sets were collected in real time and were either analyzed on-line or stored on videotape and later photographed.
23. O. T. Jones *et al.*, unpublished observations.
24. In addition, biotin–ω-CgTx and TmRhd–ω-CgTx label the same site; labeling of neurons with biotin–ω-CgTx was completely blocked by 200 n*M* TmRhd–ω-CgTx. Therefore, the more widespread channel distribution seen with biotin–ω-CgTx compared to TmRhd–ω-CgTx is due to technical aspects of the visualization, such as limited dynamic range and resolution of the camera, the small diameter of the dendrites relative to the imaging pixel size [K. R. Spring and R. J. Lowy, in *Methods in Cell Biology; Fluorescence Microscopy of Living Cells in Culture*, Y.-L. Wang and D. L. Taylor, Eds. (Academic Press, New York, 1989), vol. 29, pp. 269–289; P. J. Sammak and G. G. Borisy, *Nature* **332**, 724 (1988)] and the amplification and sensitivity of detection afforded by silver enhanced–colloidal gold and circular dityndallism microscopy [M. Hoefsmit, C. Korn, N. Blijlever, J. S. Ploem, *J. Microscopy* **143**, 161 (1986); M. De Waele, W. Renmans, E. Segers, K. Jochmans, B. Van Camp, *J. Histochem. Cytochem.* **36**, 679 (1988); S. Inoúe, A. S. Bajer, J. Mole-Bajer, *J. Cell Biol.* **91**, 321a (1981)], rather than differences in specificities of the two probes.
25. D. L. Kunze, unpublished observations.
26. K. J. Angelides, unpublished observations.
27. Fluorescence photobleach recovery measurements were made with the instrument described (*28*). The diffusion coefficient (*D*) and the mobile fraction (*f*) was determined by curve-fitting procedures (*28*). Incomplete recovery was interpreted to indicate immobility ($D \leq 3 \times 10^{-12}$ cm^2/s) of a fraction of labeled channels on the time scale of the experiment.
28. K. J. Angelides, L. W. Elmer, D. Loftus, E. Elson, *J. Cell Biol.* **106**, 1911 (1988).
29. J. L. Velazquez, C. L. Thompson, E. M. Barnes, K. J. Angelides, *J. Neurosci.*, in press.
30. L. M. Masukawa and D. A. Prince, *ibid.* **4**, 217 (1984); C. D. Woody, E. Gruen, K. McCarley, *J. Neurophysiol.* **51**, 925 (1984); R. Llinás and M. Sugimori, *J. Physiol. (London)* **305**, 171 (1980).
31. W. N. Ross and R. Werman, *J. Physiol. (London)* **389**, 319 (1987); D. W. Tank, M. Sugimori, J. A. Connor, R. R. Llinás, *Science* **242**, 773 (1988).
32. R. K. Small, M. Blank, R. Ghez, K. H. Pfenninger, *J. Cell Biol.* **98**, 1434 (1984).
33. L. Davis, G. A. Banker, O. Steward, *Nature* **330**, 477 (1987); C. C. Garner, R. P. Tucker, A. Matus, *ibid.* **336**, 674 (1988).
34. Y. Srinivasan, L. Elmer, J. Davis, V. Bennett, K. J. Angelides, *ibid.* **333**, 177 (1988).
35. C. G. Dotti, C. A. Sullivan, G. A. Banker, *J. Neurosci.* **8**, 1454 (1988).
36. We gratefully acknowledge the assistance of G. Schuster in providing the hippocampal neurons. Antibodies to MAP-2 were a gift from R. Vallee. We are indebted to J. Kirkpatrick for the use of image analysis equipment and J. Heath for the use of the Zeiss Axiophot fluorescence microscope. This work was supported by grant NS24606 and a Research Career Development Award NS01218 to K.J.A. and grant NS23573 to D.L.K. and with funds from the Biomedical Support Research Grant to O.T.J.

7 December 1988; accepted 30 March 1989

The Neuronal Growth-Associated Protein GAP-43 Induces Filopodia in Non-Neuronal Cells

MAURICIO X. ZUBER, DANIEL W. GOODMAN, LARRY R. KARNS,* MARK C. FISHMAN

The neuron-specific protein GAP-43 is associated with the membrane of the nerve growth cone and thus may be important to the activity of this distinctive neuronal structure. Transient transfection of COS and NIH 3T3 cells with appropriate vectors resulted in expression of GAP-43 in these non-neuronal cells; as in neurons, transfected GAP-43 associated with the membrane. In addition, many long fine filopodial processes extended from the periphery of such transfected cells. Stable CHO cell lines expressing GAP-43 also exhibited processes that were more numerous, far longer, and more complex than those of CHO cell lines not transfected or transfected with control plasmids. Thus GAP-43 may directly contribute to growth cone activity by regulating cell membrane structure and enhancing extension of filopodial processes.

THE PROTEIN GAP-43 IS NEURON-specific and is associated with the membrane of growth cones. Although its specific cellular function is unknown, it has been proposed to be important to growth cone function during development and to the remodeling of neuronal connections in the adult. Evidence in support of such a role for GAP-43 includes (i) the coincident expression of GAP-43 with periods of axonal elongation and regeneration in both mammals and amphibia, and with neurite growth in PC12 cells (*1, 2*); (ii) transport to, and enrichment of, the protein on membranes of the growth cone (*3*); (iii) persistence of GAP-43 expression in regions of the adult central nervous system believed to be important in learning and memory (*4, 5*); and (iv) changes in the phosphorylation state of GAP-43 in association with long-term potentiation (*6*). This protein has also been postulated to play a role in signal transduction at the membrane by binding calmodulin (*7*) and regulating the synthesis of phosphatidylinositol 4,5-bisphosphate (*8*).

To test the hypothesis that GAP-43 regulates growth cone function, we introduced expression vectors encoding rat GAP-43 into non-neuronal cells. In such cells the function of GAP-43 might be more easily

Developmental Biology Laboratory, Massachusetts General Hospital Cancer Center, and the Howard Hughes Medical Institute, Massachusetts General Hospital, Boston, MA 02114, and Harvard Medical School, Boston, MA 02115.

*Present address: Cardiovascular Research Institute, University of California, San Francisco, San Francisco, CA 94121.

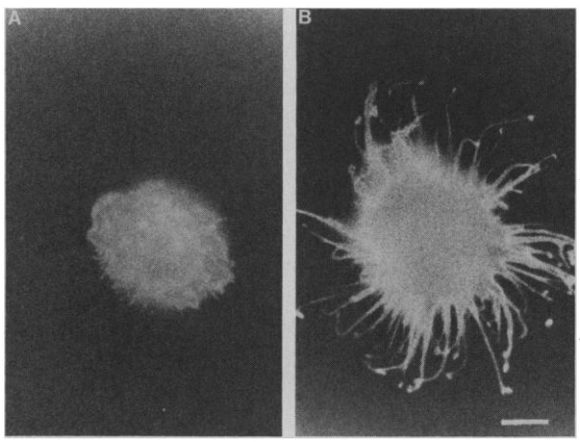

Fig. 1. Immunofluorescence of COS-7 cells transfected with (**A**) CD8 or (**B**) GAP-43. Mock-transfected cells or cells transfected with CD8 were generally round after plating, although some had a few short processes. Process extension, as from the cell in (B), was only seen in cells expressing large amounts of GAP-43, although there was a spectrum of shapes for those cells with GAP-43; some cells had smaller, longer, or fewer processes than the cell shown here, and some cells did not appear different from control cells. Bar, 10 μm. The expression vectors contained the cytomegalovirus promoter with either rat GAP-43 or CD8. The GAP-43 expression plasmid (CDM8-GAP) was constructed by inserting rat GAP-43 coding sequences (*14*) at the Xba I site of the plasmid pCDM8 (*15*). This plasmid contains the cytomegalovirus promoter, the simian virus 40 polyadenylation signal and origin of replication, and the polyoma virus origin of replication. The expression vector encoding CD8 was of similar construction (*16*). Cells were transfected by DEAE-dextran (*17*). After 48 hours the cells were passed by trypsinization and plated on cover slips coated with poly-D-lysine (0.1 μg/μl). The cells were fixed in 3.7% formaldehyde 1 hour after plating. Cover slips were incubated for 1 hour in 1% normal goat serum in phosphate-buffered saline and then incubated with either rabbit antibody to GAP-43 (*5*) or the monoclonal antibody OKT8 to CD8 (American Type Culture Collection). Appropriate secondary goat antibodies labeled with fluorescein isothiocyanate (Cooper Biomedical) were used to detect immune complexes.

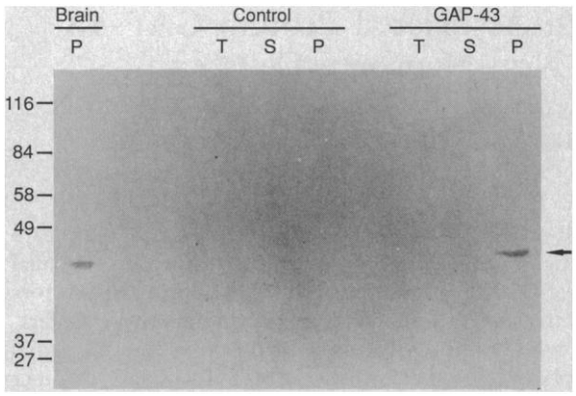

Fig. 2. Protein blot analysis of GAP-43 in CHO cell lines. GAP-43 is detected in the membrane pellet of whole newborn rat brain (Brain, P) and in the membrane pellet fraction of the GAP-43 expressing CHO cell line 5E4 (GAP-43, P). GAP-43 is not detected in any fraction of the control line P1A. GAP-43 is not detected in the total cellular homogenate of the GAP-43–expressing line because it is diluted in total cellular protein. Similar amounts of GAP-43 are present in the GAP-43 CHO cells and in brain membranes. Tissue or cells were homogenized in 0.32*M* sucrose and 10 m*M* Hepes, *p*H 7.4. These homogenates (T) were centrifuged at 1500*g* for 10 min, and the pellet was discarded. The supernatants were centrifuged at 100,000*g* for 1 hour to separate the membrane fractions (P) away from the cytosolic supernatant fractions (S). Protein (60 μg) was loaded in each lane. Clonal cell lines constitutively expressing GAP-43 were established after cotransfection of CDM8-GAP and pK0-neo, a neomycin resistance expression plasmid (*18*), into CHO cells by the calcium phosphate coprecipitation method (*19*) with the use of active Geneticin (400 μg/ml) (Gibco) for selection. For control cell lines the plasmid pCDM8 (*15*) was used instead of CDM8-GAP. Molecular weight markers are in kilodaltons and the position of GAP-43 is indicated by the arrow.

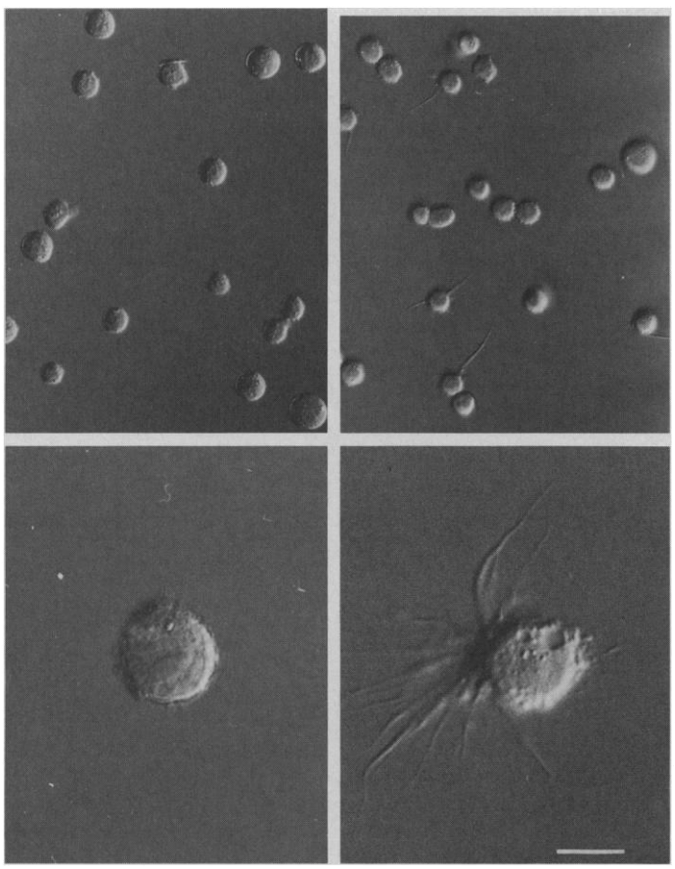

Fig. 3. Expression of GAP-43 causes changes in CHO cell shape. Micrographs were obtained with Nomarski optics of CHO cells stably transfected with CDM8 (left panels) or CDM8-GAP (right panels). Control cells were essentially round, whereas 5 of 19 cells expressing GAP-43 formed long filopodia. A field of cells is shown in the top panels, and individual cells are shown at higher magnification in the lower panels. Bar indicates 10 μm for the bottom panels and 40 μm for the top panels. After cells achieved confluency they were passed with trypsin and plated on poly-D-lysine–coated glass cover slips. Control cell lines are P1B (top left) and P2A (bottom left), and GAP-43–expressing CHO cell line is 14 (both right panels).

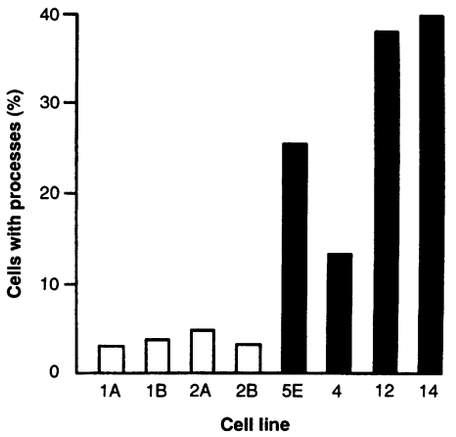

Fig. 4. Effect of GAP-43 on process formation in CHO cell lines. Cell lines were obtained as described in the legend to Fig. 2. The percentage of cells with processes in CDM8-transfected lines (control) (open bars) and GAP-43–expressing lines (solid bars) was assayed by plating CHO cells onto poly-D-lysine–coated cover slips. Cells with processes longer than 20 μm were scored as positive. To ensure comparability all assays were performed 30 to 45 min after plating, although processes could be seen for several hours. All cells examined were included, and the number of cells counted for the different lines was: 1A, 406; 1B, 408; 2A, 287; 2B, 303; 5E, 234; 4, 333; 12, 156; and 14, 161. The proportion of cells with processes in GAP-43–expressing cell lines was significantly greater than in controls ($P < 0.001$) as determined by one-tailed t test.

defined because of the absence of endogenous GAP-43 and other neuron-specific molecules. Expression vectors containing rat GAP-43 cDNA (legend to Fig. 1), or cDNA encoding the T cell–specific membrane protein CD8 (*9*) as a control, were used to transfect COS 7 cells (*10*). Cells transfected with the vector containing CD8 cDNA were analyzed by immunofluorescent labeling with a monoclonal antibody to CD8. Cells transfected with GAP-43 cDNA were examined with a rabbit antibody to GAP-43 (*5*). In both cases immunoreactivity was detected in 5 to 20% of the cells, depending on transfection efficiency, and appeared to be membrane-associated. Cells expressing CD8 were as intensely labeled as those expressing GAP-43. However, COS 7 cells expressing CD8 were essentially round (Fig. 1A), whereas many cells expressing GAP-43 had a distinctive structure with processes extending from the cell perimeter (Fig. 1B). Long, thin processes were associated only with cells expressing a large amount of GAP-43. A similar association of process outgrowth with GAP-43 expression was found when WOP cells [3T3 cells expressing polyoma T antigen (*11*)] were transfected with CDM8-GAP, a GAP-43 expression vector that included the polyoma virus origin of replication (legend to Fig. 1). In these transient transfection assays, however, the efficiency of transfection and amount of expressed protein vary, making quantitation difficult.

To overcome these problems we generated a series of clonal, stably transformed CHO cell lines that constitutively expressed GAP-43. Control cell lines were also established. The four cell lines that expressed the highest amount of GAP-43, as determined by protein blotting (Fig. 2), and four control cell lines were further analyzed.

Cells were examined by Nomarski optics immediately after plating and for several hours thereafter. Control cells were generally found to be round throughout this period (Fig. 3, left panels). On the other hand, cells expressing GAP-43 extended filopodial processes that were narrow and between 20 and 75 μm in length (Fig. 3, right panels).

Filopodia were evident as early as the first observation time point (about 10 min) and persisted for 2 to 4 hours, after which period they became less evident as the spreading cell perimeter extended to encompass them. In both control cell lines and those expressing GAP-43, the cell perimeter often exhibited broad, thin, ruffled lamellipodia (Fig. 3).

Process formation from four independent cell lines transfected with a control plasmid and four independent lines expressing the highest amounts of GAP-43 was determined. All four GAP-43 lines expressed similar levels of GAP-43 by protein blot analysis. All CHO cell lines expressing GAP-43 had a greater tendency to extend processes than did control cell lines (Fig. 4). Whereas 14 to 40% of cells expressing GAP-43 had processes longer than 20 μm, only 3 to 5% of control cells had processes of this length. In addition, 6 to 11% of cells expressing GAP-43 had multiple processes and only 0.5 to 1% of control cells showed this feature. The lengths of the processes in cells expressing GAP-43 also exceeded those in control cells.

One interpretation of our data is that GAP-43 contributes a uniquely neuronal structure to these non-neuronal cells. A more likely explanation, however, is that GAP-43 interacts with general mechanisms that control cell shape (*12*) and thereby enhances filopodial extension. Many cells can extend filopodia or lamellipodia, depending upon several factors, including the phase of the cell cycle, plating conditions, and second messenger concentrations (*13*). Thus, although cells that have GAP-43 tend to have more filopodia, this does not prove that GAP-43 plays an identical role in neurons. Such a role does not seem unreasonable however, given that the movement of growth cones is likely mediated by mechanisms such as cortical actin flow and selective adhesion, which are general means to impart cellular motion (*12*).

It has been inferred from the localization and regulation of GAP-43 that this protein is important to nerve terminal plasticity. Our results are consistent with a model whereby GAP-43 controls the dynamics of the nerve terminal membrane structure during growth. This system additionally provides a bioassay that may be used to dissect functional regions of GAP-43 and to determine how the protein may interact with second messengers and the cytoskeleton to cause this particular membrane activity.

REFERENCES AND NOTES

1. J. H. P. Skene and M. Willard, *J. Cell Biol.* **89**, 86 (1981); *ibid.*, p. 96; L. I. Benowitz, V. E. Shashoua, M. G. Yoon, *J. Neurosci.* **1**, 300 (1981); K. F. Meiri, M. Willard, M. I. Johnson, *ibid.* **8**, 2571 (1988); GAP-43 is also known as B-50, F1, pp46, and P-57. For reviews see L. I. Benowitz and A. Routtenberg [*Trends Neurosci.* **10**, 527 (1987)] and M. C. Fishman [in *Assembly of the Nervous System*, L. Landmesser, Ed. (Liss, New York, in press)].
2. H. F. Federoff, E. Grabczyk, M. C. Fishman, *J. Biol. Chem.* **263**, 19290 (1988).
3. F. Katz, L. Ellis, K. H. Pfenninger, *J. Neurosci.* **5**, 1402 (1985); P. N. E. DeGraan *et al.*, *Neurosci. Lett.* **61**, 235 (1985); K. F. Meiri, K. H. Pfenninger, M. B. Willard, *Proc. Natl. Acad. Sci. U.S.A.* **83**, 3537 (1986); J. H. P. Skene *et al.*, *Science* **233**, 783 (1986).
4. A. Rosenthal *et al.*, *EMBO J.* **6**, 3641 (1987); L. I. Benowitz, P. J. Apostolides, N. Perrone-Bozzozero, S. P. Finklestein, H. Zwiers, *J. Neurosci.* **8**, 339 (1988); R. L. Neve, E. A. Finch, E. D. Bird, L. I. Benowitz, *Proc. Natl. Acad. Sci. U.S.A.* **85**, 3638 (1988); S.-C. Ng, S. M. de la Monte, G. L. Conboy, L. R. Karns, M. C. Fishman, *Neuron* **1**, 133 (1988).
5. S. M. de la Monte, H. F. Federoff, S.-C. Ng, E. Grabczyk, M. C. Fishman, *Dev. Brain Res.*, in press.
6. R. F. Akers and A. Routtenberg, *J. Neurosci.* **7**, 3976 (1987).
7. K. A. Alexander, B. T. Wakim, G. S. Doyle, K. A. Walsh, D. R. Storm, *J. Biol. Chem.* **263**, 7544 (1988); T. J. Andreasen, C. W. Luetje, W. Heideman, D. R. Storm, *Biochemistry* **22**, 4615 (1983).
8. C. O. M. Van Hoof, P. N. E. De Graan, A. B. Oestreicher, W. H. Gispen, *J. Neurosci.* **8**, 1789 (1988).
9. B. Seed and A. Aruffo, *Proc. Natl. Acad. Sci. U.S.A.* **84**, 3365 (1987).
10. Y. Gluzman, *Cell* **23**, 175 (1981).
11. G. Della-Valle, R. Fenton, C. Basilico, *Mol. Cell. Biol.* **1**, 418 (1981).
12. D. Bray and J. G. White, *Science* **239**, 883 (1988); S. J. Smith, *ibid.* **242**, 708 (1988); J. P. Trinkuns, in *Biology of the Nerve Growth Cone*, S. Kater and P. Letourneau, Eds. (Liss, New York, 1988), pp. 1–19.
13. L. E. Allred and K. R. Porter in *Surfaces of Normal and Malignant Cells*, R. O. Hynes, Ed. (Wiley, New York, 1979), pp. 21–32.
14. L. R. Karns, S.-C. Ng, J. A. Freeman, M. C. Fishman, *Science* **236**, 597 (1987).
15. B. Seed, *Nature* **329**, 840 (1987).
16. ——— and A. Aruffo, personal communications.
17. M. X. Zuber, E. R. Simpson, M. R. Waterman, *Science* **234**, 1258 (1986).
18. K. Van-Doren, D. Hanahan, Y. Gluzman, *J. Virol.* **50**, 607 (1984).
19. F. M. Ausubel *et al.*, Eds., *Current Protocols in Molecular Biology* (Green Publishing Associates/Wiley-Interscience, New York, 1987), vol. 1, pp. 9.0.1–9.5.6.

20. We thank B. Seed for the plasmid pCDM8, C. Basilico for the WOP cells, and J. Jackson for preparation of the manuscript. M.X.Z. is the recipient of a postdoctoral fellowship from the American Cancer Society and D.W.G. has partial support from an Institutional Physician Scientist Award from NIH.

18 November 1988; accepted 8 March 1989

Three-Dimensional Structure of Human Serum Albumin

DANIEL C. CARTER,* XIAO-MIN HE, SIBYL H. MUNSON, PAMELA D. TWIGG, KIM M. GERNERT, M. BETH BROOM, TERESA Y. MILLER

The three-dimensional structure of human serum albumin has been solved at 6.0 angstrom (Å) resolution by the method of multiple isomorphous replacement. Crystals were grown from solutions of polyethylene glycol in the infrequently observed space group $P42_12$ (unit cell constants $a = b = 186.5 \pm 0.5$ Å and $c = 81.0 \pm 0.5$ Å) and diffracted x-rays to lattice *d*-spacings of less than 2.9 Å. The electron density maps are of high quality and revealed the structure as a predominantly α-helical globin protein in which the course of the polypeptide can be traced. The binding loci of several organic compounds have been determined.

THE SERUM ALBUMIN PROTEINS ARE among the most highly studied and applied in biochemistry (*1–4*). These proteins possess high helical content and high cysteine content (17 disulfides), and have approximate molecular weights of 65 kD. Human serum albumin (HSA) comprises 585 amino acids with a molecular weight of 66,500 daltons. Complete amino acid sequences are known for HSA (*5*) and for bovine and rat serum albumins (*6, 7*). Comparisons of these amino acid sequences reveal high sequence homology. The serum albumins also possess internal sequence homology in the form of three tandem gene duplications (hereafter referred to as domains I, II, and III). In addition to three tandem gene duplications, there may be as many as six repeating structural motifs based on the position and frequence of the exon junctures (*8*). Although the principal function of serum albumin remains disputed, as the most abundant plasma protein of the circulatory system it contributes significantly to colloidal osmotic blood pressure and to many transport and regulatory processes. A number of studies have focused on the multifunctional binding properties of serum albumin. This protein binds a wide variety of substrates, ranging from metals such as calcium and copper to fatty acids, amino

National Aeronautics and Space Administration, Space Sciences Laboratory, Code ES76 Biophysics Branch, Marshall Space Flight Center, AL 35812.

*To whom correspondence should be addressed.